Int J Thermophys (2010) 31:1896–1903
DOI 10.1007/s10765-008-0542-6

A Digital Variable-Angle Rolling-Ball Viscometer for Measurement of Viscosity, Density, and Bubble-Point Pressure of CO_2 and Organic Liquid Mixtures

Yoshiyuki Sato · Hiroki Yoshioka · Shohei Aikawa · Richard Lee Smith Jr.

Published online: 16 December 2008
© Springer Science+Business Media, LLC 2008

Abstract A new apparatus was developed for measuring the viscosity, density, and bubble-point pressure of CO_2 and organic liquid mixtures. The apparatus is based on the rolling-ball principle and consists of a computer-controlled stepper motor that rotates a high-pressure cell that is equipped with a sapphire window, a movable piston, and a position-sensing device. Design of the high-pressure cell was made such that compositions could be determined by mass. The viscosity was determined by sensing the speed of a rolling ball, and the density was determined by sensing the position of the piston with a linear-variable differential transformer. Bubble-point pressures were measured with the synthetic method. The viscosity and density of octane and decane were measured, and the average deviations of these properties compared with reliable literature values were 1.1 % and 0.15 %, respectively. The viscosity and density of CO_2 + tetrahydrofuran system were measured at a temperature of 60 °C, a pressure of 10.2 MPa, and CO_2 mole fractions up to 0.3. Bubble-point pressures for the CO_2 + tetrahydrofuran system were in good agreement with literature data.

Keywords Viscosity · Density · Bubble-point pressure · CO_2 expanded liquid

1 Introduction

In Asia, there is a large effort to monitor the emissions of SO_2, NO_x, CO, non-methane volatile organic compounds (NMVOCs), black carbon, and organic carbon. In the conclusions of one study [1], the amount of NMVOCs in 2020 is expected to be increase by as much as 40 % on average over 2000 levels, with some countries forecasted to

Y. Sato (✉) · H. Yoshioka · S. Aikawa · R. L. Smith Jr.
Research Center of Supercritical Fluid Technology, Graduate School of Engineering, Tohoku University, Aoba 6-6-11, Aramaki, Aoba-ku, Sendai 980-8579, Japan
e-mail: ysato@scf.che.tohoku.ac.jp

have an increase in NMVOC emissions approaching 100 % [1] by 2020. The chief sources of the NMVOC emissions are stationary combustion, transportation, solvent use (not paint), paints and coatings, chemical processing, etc. Because of its probable future impact, organic solvent reductions in the paint and coatings industry are an attractive target, since emissions from these sources are expected to rise and there is sufficient industrial interest to search for alternative solvents.

Paints and coatings consist of mainly a polymer, pigments, a binder, and a large amount of volatile organic compounds (VOC) that give the mixture fluidity. The VOCs serve as the vehicle for transporting the solids and also act to reduce the viscosity of the mixture. The VOCs are also chosen to provide desired drying times and hence the desired finish. One proposal being studied for paints and coatings is to use a gas at high pressure, such as CO_2, in order to adjust the viscosity of the coating and drying times and thus to allow the reduction and possible elimination of the organic solvent. However, data to consider such proposals are scarce, and one of the reasons for this is the lack of suitable apparatus for measuring the viscosities and properties of the mixtures.

In considering the painting or coating of any substrate, the viscosity, density, surface tension, and the general thermodynamic condition of the mixture are important for process design and control of the coating thickness. In this study, a new apparatus was developed for measuring the viscosity, density, and bubble-point pressure of high-pressure gas and organic liquid mixtures. Calibration of the viscometer and confirmation of viscosity, density, and bubble-point pressure measurements are reported. Several data are reported for the CO_2 and tetrahydrofuran system due to its importance in some technological coatings.

2 Experimental

A schematic diagram of the apparatus is shown in Fig. 1. The specific features of the rolling-ball viscometer are digital angular positioning of the cell via a computer-controlled stepper motor (Oriental Motor Co. Ltd., ASM46AA-T20), a cell body that is constructed from light-weight titanium (JIS Class 2), a movable piston with position sensing by a linear-variable differential transformer (LVDT) (Shinko Denshi Co. Ltd., WA-2S and A22-3), and a sapphire window for visual observation. The apparatus uses the rolling-ball principle for measurements, since this method allows for the study of both low- and high-pressure measurements [2], and its principle has been confirmed for both paint and coating mixtures [3], CO_2 containing mixtures [4,5], and fluid mixtures at high pressures [6–8]. The digital angular positioning of the cell allows for highly reproducible initial conditions to within 0.05° to be maintained. Computer control of the apparatus allows for repetitive measurements to be made automatically or measurements of properties at an angular sequence. The light-weight cell body (ca. 390 g, inner bore of Φ 10.34 mm) makes it possible to determine mixture compositions gravimetrically. The movable piston and the sensing of its position by an LVDT allows for the volume to be detected or pressure to be varied at constant composition, and along with the window, allows the operator to observe the thermodynamic state of the mixture. Determination of the velocity of the rolling ball is accomplished by

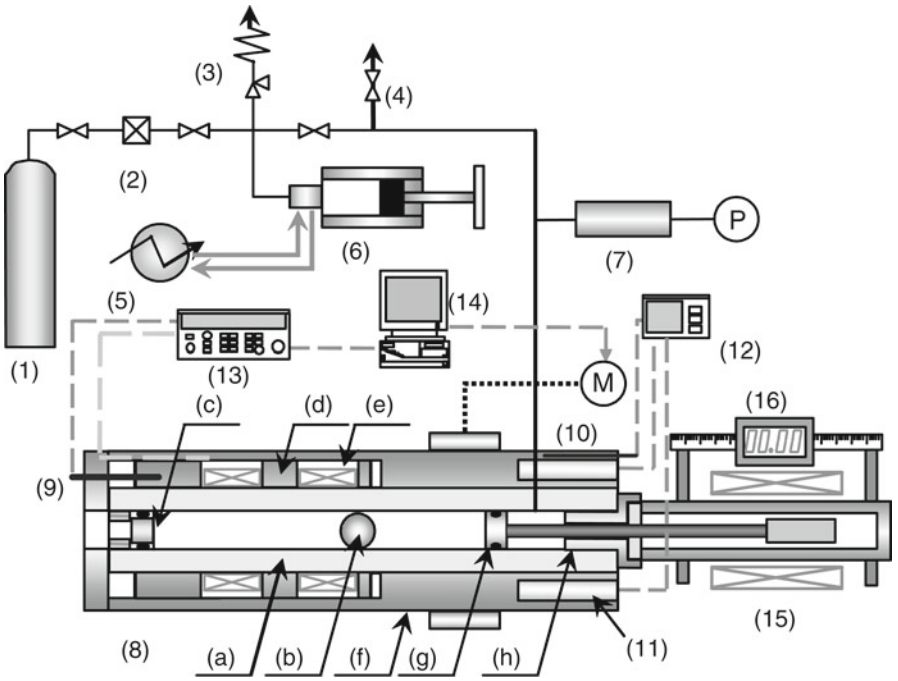

Fig. 1 Schematic diagram of the viscometer: (1) CO_2 bomb, (2) filter, (3) relief valve, (4) purge valve, (5) chiller, (6) hand pump, (7) buffer, (8) viscosity cell, (9) 4-wire Pt thermometer, (10) 3-wire Pt thermometer, (11) cartridge heater, (12) temperature controller, (13) data logger, (14) computer, (15) LVDT, (16) linear scale, (a) cell body, (b) rolling body, (c) sapphire window, (d) coil bobbin, (e) coil, (f) heating jacket, (g) piston, (h) piston gland

sensing the induced electromotive force that results when a magnetic stainless-steel ball (Misumi Corporation, SUS 440C, Φ 10.32 mm) passes through the two sets of hand-wound, balanced (clockwise, counter-clockwise) coils. Sensing of the emf was chosen due to simplicity, although it is apparent that improvements of the noise in the present measurements can be improved using an additional LVDT as shown in studies that use this type of device for determining the velocities of falling sinkers [9].

In the rolling-ball viscometer developed in this study, the viscosity, η, was obtained by measuring the rolling time, Δt, of the ball as it passed through the two coils in an inclined tube filled with the liquid sample using

$$\eta = K\,\Delta t\,(\rho_{\mathrm{b}} - \rho_{\mathrm{L}})\sin\theta \tag{1}$$

where K is an apparatus constant and θ is the inclination angle. ρ_{b} and ρ_{L} are the densities of the ball and sample liquid, respectively. The terminal velocity was confirmed through theoretical calculations for the given Reynolds number and experimental reproducibility. Viscosities were determined by calibration with toluene, since reliable viscosity data have been reported in the literatures [10,11] for this substance.

The apparatus constant, K, was determined for a given angular setting according to temperature, pressure, and mechanical dimensions at the system conditions. The

temperature and pressure dependencies of K were determined using the following relationships that describe the deformation of materials with temperature and pressure [7]:

$$\frac{K}{K_0} = 1 + \left\{\alpha_b + \alpha_t + \left(\frac{r_0}{1+r_0} - \frac{5}{2}\frac{r_0}{1-r_0}\right)(\alpha_b - \alpha_t)\right\}(T - T_0) + \left\{\beta - \kappa_b + \left(\frac{5}{2}\frac{r_0}{1-r_0} - \frac{r_0}{1+r_0}\right)(\beta + \kappa_b)\right\}(P - P_0), \quad (2)$$

$$\beta = \frac{1}{E_t}\left(\frac{r_1^2 + r_2^2 - \nu_t r_1^2}{r_2^2 - r_1^2} + \nu_t\right), \quad (3)$$

where K_0 is an apparatus constant at a given inclination angle, reference temperature, T_0 (40 °C), and reference pressure, P_0 (0.1 MPa). r_0 is the diameter ratio (d_0/D_0) of the ball to the tube at the reference condition. r_1 and r_2 are the inner and outer radii of the viscometer, α and κ are the thermal expansion and isothermal compressibility of the materials, respectively, and ν and E are the Poisson ratio and the Young's modulus, respectively, of the tube and ball materials. Subscripts t and b denote the tube (viscometer) and ball, respectively.

Densities were measured using the masses of materials loaded gravimetrically and using the piston displacement detected by the LVDT. Bubble-point pressures were determined with the synthetic method, namely, the bubble-point pressure of a mixture of known composition was observed during the movement of piston. The maximum inner volume of the cell was about 8.8 cm^3, and the displacement could be detected to within ±0.01 mm with a linear scale (Mitsutoyo Corporation, SD-10D) in conjunction with the LVDT as a null detector. The inner volume of the viscometer and cross-sectional area of the piston were calibrated with distilled water. The uncertainty of the density measurement is estimated to be 0.28 $kg \cdot m^{-3}$ (the expanded uncertainty, coverage factor is $k = 2$). The uncertainties of the pressure and temperature measurements are estimated to be within ±0.02 MPa and ±0.05 K, respectively. The temperature limit of the apparatus is 100 °C, and the design pressure limit is 15 MPa.

3 Results and Discussion

The variation of the apparatus constant K was studied as a function of temperature and pressure. The temperature and pressure dependencies of K at an inclined angle of 10° are shown in Fig. 2 along with the calculation results of Eqs. 2 and 3. Since the pressure dependence of K could not be accurately predicted with Eqs. 2 and 3, β in Eq. 3 was fitted to the experimental data. From the results in Fig. 2, it was found that Eqs. 2 and 3 could represent the temperature and pressure dependencies of the apparatus constant K to within average deviations of 0.48 % and 0.55 %, respectively.

Densities of octane, decane, and toluene were measured over a temperature range from 40 °C to 70 °C to confirm the reliability of the density measurements. Experimental densities agreed with literature values [10,11] with an average deviation of 0.15 %. The viscosities of octane and decane were measured at temperatures of 50 °C

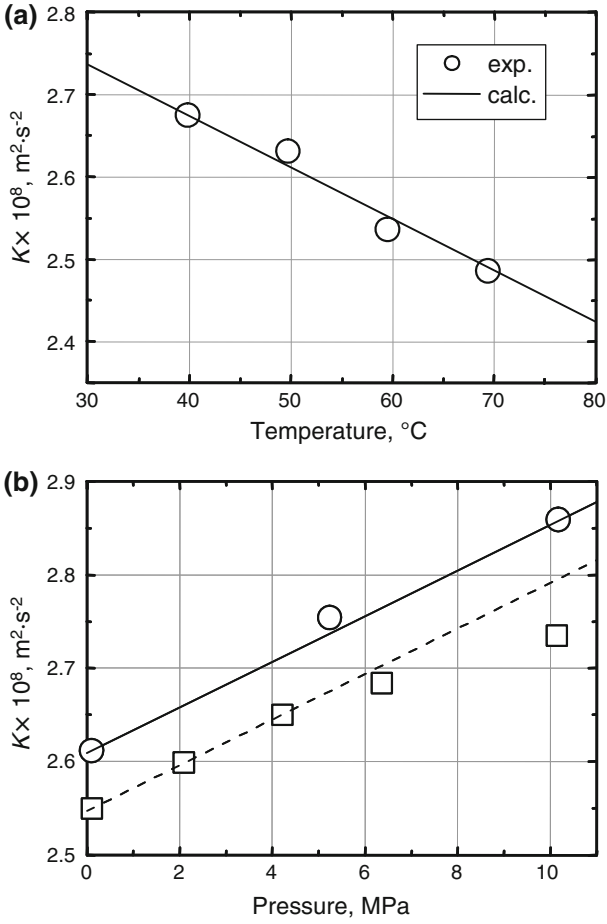

Fig. 2 (a) Temperature ($P = 0.1$ MPa) and (b) pressure (*circles* at 50 °C and *squares* at 60 °C) dependence of apparatus constant, K, at inclined angle of 10°

and 60 °C and at pressures up to 10 MPa. Experimental results for the viscosity of pure *n*-octane and pure *n*-decane (Fig. 3 and Tables 1–3) had an average deviation of 1.1 % in comparisons with literature data [12], and thus were judged to be in good agreement. However, the variation of the viscosity for ten measurements was 3.6 %, which can be attributed to the Δt measurements that showed high noise due to the low level of induced electromotive force. Improvement in the accuracy of the Δt measurement will be examined in future work.

A few data were determined that are of importance for practical paint and coating processes. Experimental results for the viscosity, density, and bubble-point pressure for the CO_2 + tetrahydrofuran system are shown in Figs. 4 and 5 and Tables 4 and 5. A number of density data are also reported by Zhang and Kiran [15]. As shown in Fig. 4 for the CO_2 + tetrahydrofuran system, the viscosity decreased with increasing CO_2 mole fraction and the density slightly increased with increasing CO_2 mole

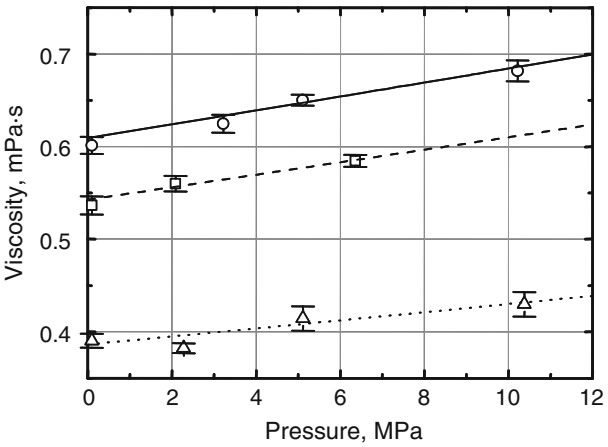

Fig. 3 Viscosities of octane and decane obtained in this study over a range of pressures compared with smoothed literature values. *Circles* represent decane at 50°C, *squares* represent decane at 60°C, *triangles* represent octane at 50°C, *lines* represent literature values [12]

Table 1 Density and viscosity of compressed liquid decane

T (K)	P (MPa)	ρ (kg · m^{-3})	η (mPa · s)
323.1	0.10	704.1	0.601
323.2	3.22	704.4	0.636
323.2	5.11	710.5	0.650
323.2	10.20	714.5	0.682
333.1	0.10	690.7	0.537
333.1	2.09	701.1	0.560
333.1	6.36	705.4	0.585

Table 2 Density and viscosity of compressed liquid octane

T(K)	P (MPa)	ρ (kg · m^{-3})	η (mPa · s)
323.2	0.18	679.0	0.391
323.2	2.28	677.1	0.382
323.2	5.12	683.8	0.414
323.2	10.38	686.9	0.430

Table 3 Density of compressed liquid toluene

T(K)	P (MPa)	ρ (kg·m^{-3})
323.2	5.24	843.3
323.2	10.20	847.8
333.1	2.09	830.7
333.1	4.22	832.7
333.1	6.36	834.8
333.1	10.20	838.2

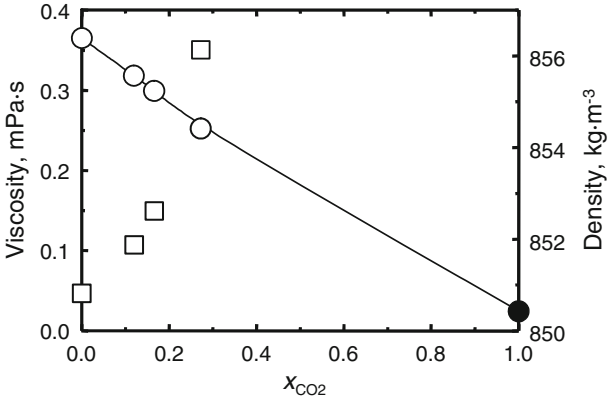

Fig. 4 Viscosities and densities of the CO_2 + tetrahydrofuran system at 60 °C and 10.2 MPa. *Circles* represent viscosity, *squares* represent density, filled circle represents literature data [13]

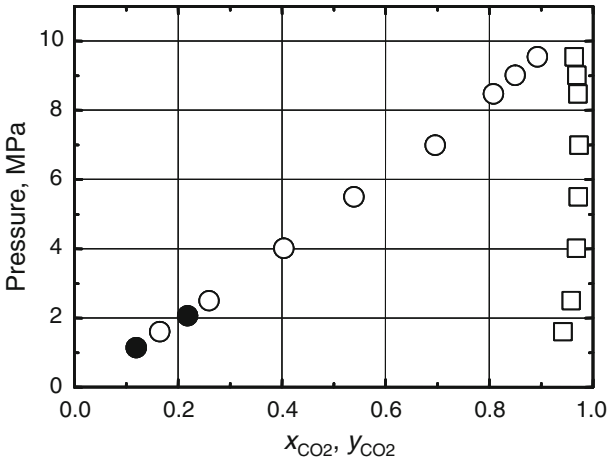

Fig. 5 Bubble-point pressures obtained for the CO_2 + tetrahydrofuran system at temperature of 60 °C compared with vapor–liquid equilibria data in the literature [14]. *Filled circles* represent this work, *unfilled circles, squares* represent literature data [14]

fraction. Remarkably, the viscosity reduction due to CO_2 showed close to a linear dependence on the CO_2 mole fraction, which means that the viscosity reduction provided by CO_2 in the organic liquid system can be calculated by a simple linear relationship. The viscosity reduction with CO_2 can be attributed to the dilution effect as dissolved CO_2 probably causes an increase in the free volume of the solution. The density increase with CO_2 can be attributed to the mixing of CO_2 with tetrahydrofuran and the increased packing of molecules.

In Fig. 5, experimental results of vapor–liquid equilibria for CO_2 + tetrahydrofuran system at 60 °C are shown. Solubilities of CO_2 in tetrahydrofuran were in good agreement with literature values [14]. The apparatus and procedures were determined to be reliable.

Table 4 Density and viscosity of carbon dioxide + tetrahydrofuran at 10.2 MPa and 333.2 K

xCO_2	ρ (kg · m^{-3})	η (mPa · s)
0	850.8	0.365
0.119	851.9	0.318
0.166	852.6	0.300
0.272	856.1	0.252

Table 5 Bubble-point pressure of carbon dioxide + tetrahydrofuran at 333.2 K

xCO_2	Bubble-point pressure (MPa)
0.119	1.14
0.219	2.06

4 Conclusions

In this study, a new apparatus was developed for viscosity, density, and vapor–liquid equilibria. Data obtained were found to be in agreement with literature results for pure component densities and the viscosities, which demonstrated the reliability of the apparatus. New experimental data of viscosity and vapor–liquid equilibria of the CO_2 + tetrahydrofuran system were obtained at 60 °C to demonstrate the operation of the apparatus. The viscosity of tetrahydrofuran mixed with CO_2 shows a simple linear dependence on the CO_2 mole fraction.

Acknowledgment The authors gratefully acknowledge support of this research from industrial sources.

References

1. Y. Matsumura, M. Sasaki, K. Okuda, S. Takami, S. Ohara, M. Umetsu, T. Adschiri, Combust. Sci. Technol. **178**, 509 (2006)
2. M.A. Hernandez-Galvan, F. Garcia-Sanchez, R. Macias-Salinas, Fluid Phase Equilib. **262**, 51 (2007)
3. B.J. Briscoe, P.F. Luckham, S.R. Ren, Colloids Surf. **62**, 153 (1992)
4. D. Tomida, A. Kumagai, K. Qiao, C. Yokoyama, J. Chem. Eng. Data **52**, 1638 (2007)
5. D. Tomida, A. Kumagai, C. Yokoyama, Int. J. Thermophys. **28**, 133 (2007)
6. E.M. Stanley, R.C. Batten, Anal. Chem. **40**, 1751 (1968)
7. M. Izuchi, K. Nishibata, Jpn. J. Appl. Phys. **25**, 1091 (1986)
8. K. Nishibata, M. Izuchi, Physica B & C **139**, 903 (1986)
9. C. Dindar, E. Kiran, Rev. Sci. Instrum. **73**, 3664 (2002)
10. M.J. Assael, N.K. Dalaouti, S. Polimatidou, Int. J. Thermophys. **20**, 1367 (1999)
11. C.M.B.P. Oliveira, W.A. Wakeham, Int. J. Thermophys. **13**, 773 (1992)
12. M.L. Huber, A. Laesecke, H.W. Xiang, Fluid Phase Equilib. **224**, 263 (2004)
13. A. Fenghour, W.A. Wakeham, V. Vesovic, J. Phys. Chem. Ref. Data **27**, 31 (1998)
14. M.J. Lazzaroni, D. Bush, J.S. Brown, C.A. Eckert, J. Chem. Eng. Data **50**, 60 (2005)
15. W. Zhang, E. Kiran, J. Chem. Thermodyn. **35**, 605 (2003)